

Experimental study on concrete columns hybrid reinforced by steel and FRP bars under seismic loading

Sun Zeyang¹ Wu Gang¹ Wang Yanhua¹ Wu Zhishen^{1,2}

(¹Key Laboratory of Concrete and Prestressed Concrete Structures of Ministry of Education, Southeast University, Nanjing 210096, China)

(²International Institute for Urban Systems Engineering, Southeast University, Nanjing 210096, China)

Abstract: In order to study the dynamic behavior of hybrid reinforced concrete columns, shaking table tests of three concrete columns with equal initial stiffness were conducted. The longitudinal reinforcements include an ordinary steel bar, a steel-fiber reinforced polymer (FRP) composite bar (SFCB), and hybrid reinforcement (steel bar and FRP bar, C-H). Test results show that the peak ground acceleration (PGA) responses of different columns are similar to each other. For an ordinary reinforced concrete (RC) column, the plastic strain of the steel bar develops rapidly after the PGA of the input ground motion reaches 100 cm/s^2 , and the corresponding residual strain develops dramatically. For a SFCB column, even after the peak strain reaches 0.015, the residual strain is below 5×10^{-4} . For the hybrid column C-H, the residual strain of the FRP bar is similar to that of the SFCB column. In general, concrete columns with hybrid steel and FRP bar reinforcement can achieve smaller residual deformation, and the SFCB reinforced columns can be constructed in extreme environments, such as offshore bridges, due to good anti-corrosion performance.

Key words: concrete column; shaking table test; hybrid reinforcement; peak ground acceleration; strain distribution

DOI: 10.3969/j.issn.1003-7985.2016.04.008

Economic development requires the design criterion of important structures to range from complete prevention of collapse to being post-earthquake repairable. During an earthquake, both the damage probability of a structure and the required repair time should be decreased^[1]. Based on the current research results of performance-based seismic design^[2] and the design theory regarding enhancement of the post-yield stiffness of reinforced concrete (RC) columns^[3], concrete columns reinforced by steel-fiber reinforced polymer (FRP) composite

bars (SFCBs)^[4] were proposed by our research group. The SFCB was made of an inner steel bar and an outer covering of the longitudinal FRP, and the factory products were successfully manufactured by modifying the pultrusion equipment of the FRP bar. A large number of mechanical tests of SFCB have been conducted, and the stress-strain mode of the SFCB has been improved^[5]. The static behaviors of concrete beams and concrete columns reinforced by SFCB have also been conducted^[6-8].

The shaking table test may best reflect the dynamic performance of a concrete structure^[9-10]. To study the response characteristics of hybrid reinforced columns under simulated ground motions, three concrete columns were cast based on the simulation results^[11]: longitudinal reinforcement including an ordinary steel bar, a hybrid steel/FRP bar, and a SFCB.

1 Shaking Table Test Design

1.1 Specimen parameters

To characterize the mechanical properties of an SFCB and the corresponding concrete column, the post-yield stiffness ratio of SFCB r_{sf} (without considering the contribution of the resin in SFCB) can be calculated as follows:

$$r_{sf} = \frac{E_f A_f}{E_s A_s + E_f A_f}$$

where E_s and A_s are the elastic modulus and the total area of the steel bar, respectively; E_f and A_f are the elastic modulus and the area of the FRP bar or the SFCB's outer FRP, respectively. The section equivalent reinforcement ratio ρ_{sf}^e can be expressed based on the elastic modulus of a steel bar:

$$\rho_{sf}^e = \frac{E_f A_f}{r_{sf} E_s A_g}$$

where A_g is the gross area of the column section.

According to the principle of the equivalent reinforcement ratio, three concrete columns are designed. The mechanical properties of the longitudinal reinforcement and the column parameters are shown in Tab. 1, where C-S12 is the control column; C-H is the hybrid reinforcement by the steel bar and the ballast FRP (BFRP) bar; C-S10B85 is reinforced by SFCB with a 10 mm inner steel bar and an outer wrap of 85 bundles of basalt fibers (2 400 tex). The BFRP bars in column C-H are from the same batch as those used in S10B85.

Received 2016-07-16.

Biographies: Sun Zeyang (1984—), male, doctor; Wu Gang (corresponding author), male, doctor, professor, g.wu@seu.edu.cn.

Foundation items: The National Key Technology R&D Program of China (No. 2014BAK11B04), the National Natural Science Foundation of China (No. 51528802, 51408126), the Natural Science Foundation of Jiangsu Province (No. BK20140631).

Citation: Sun Zeyang, Wu Gang, Wang Yanhua, et al. Experimental study on concrete columns hybrid reinforced by steel and FRP bars under seismic loading[J]. Journal of Southeast University (English Edition), 2016, 32(4): 439 – 444. DOI: 10.3969/j.issn.1003-7985.2016.04.008.

Tab. 1 Specimen design and the mechanical properties of column longitudinal reinforcement

Column type		Diameter/mm	Elastic modulus/GPa	r_{sf}	Yield strength/MPa	Ultimate strength/MPa	$\rho_{sf}^o/\%$
C-S12		12	200		400	529.6	0.54
C-H	Steel bar	10	200		450	621.0	0.48
	BFRP bar	13	45.38			1 075.6	
C-S10B85		18	94.6	0.266	189.2	544.08	0.58

The test is conducted in the Key Laboratory of Concrete and Prestressed Concrete Structures of the Ministry of Education of Southeast University. The size of the shaking table is 4 m × 6 m; the maximum horizontal exciting force is 100 t; the loading capacity of a vertical load is 30 t; and the maximum horizontal displacement is ±250 mm. Thus, the concrete column cross section is designed as 250 mm × 250 mm, and the shear span ratio λ is 5. The specimen geometrical parameters are shown in Fig. 2. To avoid shear failure, stirrup encryption requirements by the plastic hinge region are applied to the full length of the concrete column. The average tested compressive strength of the 150 mm concrete cube at 28 d is 36.64 MPa, and the corresponding cylinder compressive strength is 29.31 MPa. The concrete block on the column cap is approximately 20 t. Therefore, the axial compression ratio is 0.11.

1.2 Loading programs and measurement

The north component of the near-field earthquake EL central wave (lasts for 53.73 s, see Fig. 1) is selected as the input ground motion; the original peak ground acceleration (PGA) is 341.7 cm/s² (0.35g). In this paper, the ground motion with 50 cm/s² PGA is selected for the first loading, and the PGA increment is 20 cm/s² for each loading gradient. The vibration frequency of a specimen at different loading gradients is obtained by white-noise excitation with 40 cm/s² PGA.

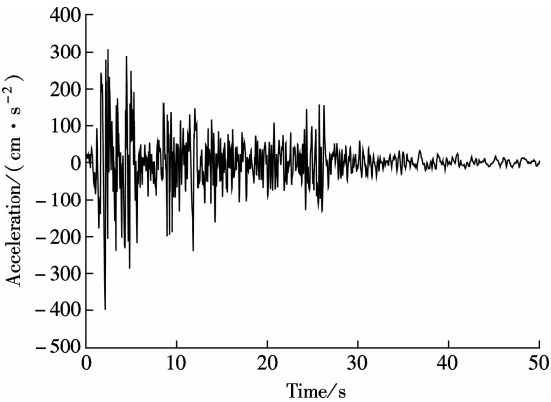


Fig. 1 EL centro earthquake

The measurements include 1) Acceleration: seven acceleration sensors are placed on the specimen (see Fig. 2(a)). Three are placed along the middle line of the column, and the other two sensors are arranged symmetrically on the concrete block weight. 2) Longitudinal reinforcement strain: seven strain gauges (spacing 80 mm, see Fig. 2(b)) are placed on each longitudinal bar. Two are below the interface between the column base and anchorage zone, and the other five strain gauges are in the plastic hinge region. The dimension of each strain gauge is 3 mm × 5 mm, and the surface of the reinforcement is rubbed with sandpaper to enhance the interface. For C-H, the strain gauges are placed on both the steel bar and the FRP bar.

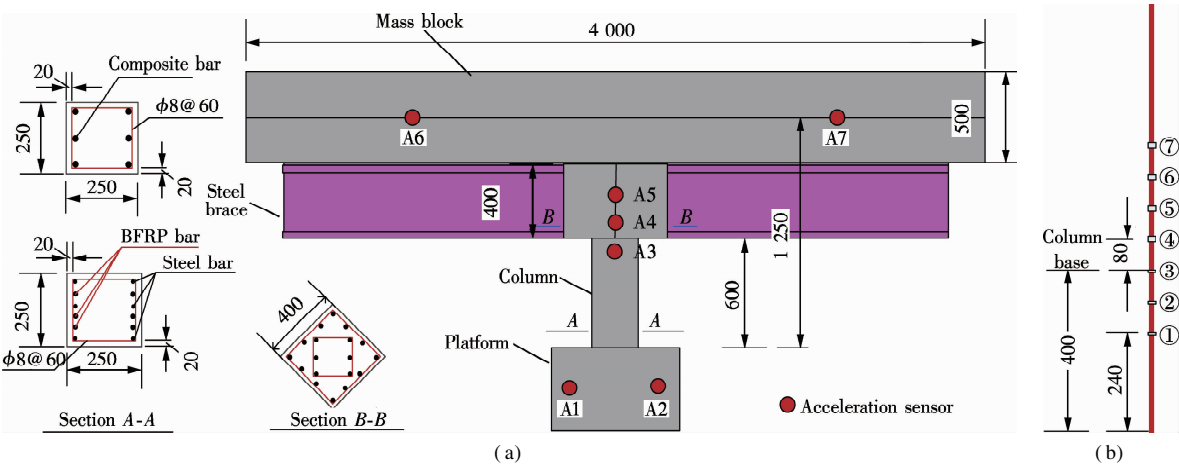


Fig. 2 Specimen geometry and location of strain gauges(units: mm). (a) Specimen geometry; (b) Location of strain gauges

2 Test Results

2.1 Test phenomenon

The initial natural frequency of C-S12 before cracking is 2.32 Hz. When the PGA of the input ground motion is

60 cm/s², the natural frequency reduces to 1.95 Hz (decrease of 19%) after cracking, but there is no residual crack observed because of the weight of the concrete block. When the earthquake PGA reaches 120 cm/s², corner concrete partial spalling and two residual cracks are found within the region of 100 to 150 mm from the column

base. When the PGA reaches 160 cm/s^2 , the vertical residual cracks at the concrete cover can be observed. Much of the corner concrete crushes when the input PGA is 360 cm/s^2 ($0.37g$), and the main region of the crushed concrete is located within the range from 50 to 150 mm above the column platform, as shown in Fig. 3(a). After the PGA reaches 380 cm/s^2 ($0.39g$, approximately the intensity of major earthquake in the 8-degree seismic fortification region in China, GB50011—2010), more concrete spalling is observed, and the corresponding natural frequency is 1.13 Hz . The test is stopped at this loading gradient.

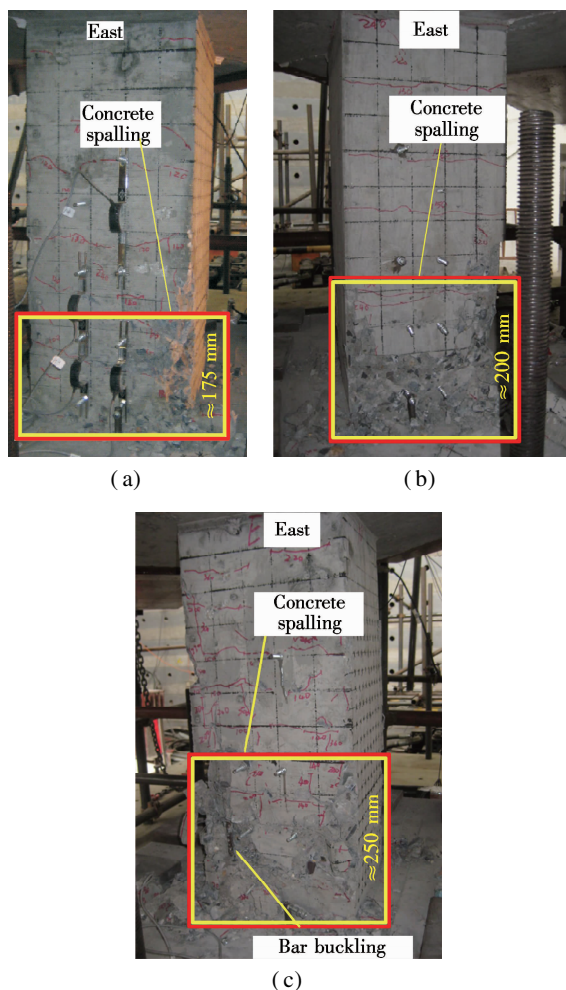


Fig. 3 Specimens' failure patterns when the PGA of the input wave stopped increasing. (a) C-S12; (b) C-S10B85; (c) C-H

For column C-S10B85, since the obtained frequency is abnormal, the stable natural frequency in the initial loading stage is 2.17 Hz , i. e., slightly lower than the first frequency of 2.32 Hz . In this case, minor cracks may have been formed. When the loading PGA reaches 100 cm/s^2 , seven flexural cracks are found to be evenly distributed along the specimen, and the corresponding natural frequency is reduced to 1.83 Hz . When the loading PGA is 200 cm/s^2 , concrete at the column base is moderately crushed (the natural frequency is 1.43 Hz). When the input PGA increases to 380 cm/s^2 , the concrete cover ex-

hibited partial spalling; the natural frequency reduces to 1.22 Hz , and the number of cracks remains almost the same as in the former loading. When the input PGA is 440 cm/s^2 ($0.45g$), a large amount of the concrete cover is crushed, as shown in Fig. 3(b), and the corresponding natural frequency is 1.06 Hz .

When the input PGA of C-H is 80 cm/s^2 , two residual cracks appears at the loading actuator side (west side), 250 mm from the column platform. On the east side of C-H, two slight residual cracks are observed 75 and 260 mm above the column platform, demonstrating the lower crack resistance capacity of C-H. Based on the subsequent white-noise excitation, the vibration frequency decreases from 2.19 to 1.64 Hz . A clearly visible residual crack is observed at the column base when the input PGA is 100 cm/s^2 . When the input PGA is 120 cm/s^2 , the natural frequency slightly decreases to 1.61 Hz ; however, six new residual cracks are observed on the west side (see Fig. 3(c)), and a small number of vertical cracks are found at the column corner. When the input PGA reaches 160 cm/s^2 , spalling of the edge of the concrete cover occurs, and the corresponding natural frequency is 1.19 Hz . The test stops after the PGA reaches 560 cm/s^2 ($0.57g$), at which point spalling of much of the corner concrete occurs, as shown in Fig. 3(c). The longitudinal steel bar buckles, while the FRP bars unbuckle.

2.2 Relative acceleration response

The benefit of the shaking table test is that it can capture the time difference between the absolute PGA responses. Taking C-H as an example, the time differences of the PGA responses among A1 to A5 are mainly at 0.03 s , whereas the absolute PGA of the mass block is delayed in the range of 1.22 to 1.29 s . The relative acceleration response (RAR), which is the difference between the absolute acceleration of the column cap and that of the column platform, reflects the actual internal force of the concrete column. The RARs of the three columns are shown in Fig. 4.

The RAR increases with the increase of distance from the column platform, wherein the relative PGA (RPGA) recorded by the three acceleration sensors at A3, A4, and A5 linearly increases with the increase of the sensor's location. With the increase of the input PGA, the absolute PGA of the concrete block reduces from the maximum to the minimum, whereas the relative PGA remains at the maximum; this behavior is consistent with the response mechanism of a column under an earthquake.

The RPGA responses of different concrete columns at close positions are similar to each other when the input PGAs are similar. Before the input PGA reaches 400 cm/s^2 , the RARs are substantially linear as a function of the input PGA. After the input PGA reaches 450 cm/s^2 , the RPGA does not change significantly with the increase of

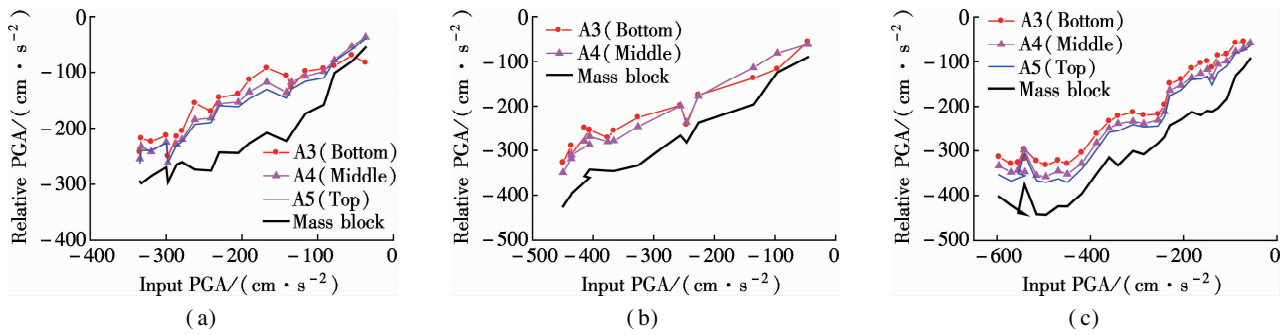


Fig. 4 Relative PGA responses of the concrete columns at the input wave's negative side. (a) C-S12; (b) C-S10B85; (c) C-H

the input PGA, exhibiting a plateau-like response as a function of the input PGA. The corresponding experimental phenomenon is the absorption of input energy via steel buckling. Note that the FRP bar exhibits no fracture and no buckling, demonstrating that the C-H can have smaller residual deformation after a major earthquake.

2.3 Strain response

From the strain gauges in the anchorage zone, when the input PGA is between 140 and 160 cm/s^2 , the residual strains of C-S12 on both sides A and B are compressive strain (see Fig. 5). In addition, the residual strain in the region of 100 to 200 mm from the column platform is also compressive strain, and the value of the residual compressive strain on side A is much greater than that on side B. This response occurs due to the following reasons: 1) After cracking, the residual compressive strains on sides A and B are caused by the concrete block; 2) During the input ground motion, the peak tensile and compressive strain on side A is much larger than that on side B, and the concrete on side A has greater damage than that at side B, leading to the larger residual compressive strain on side A.

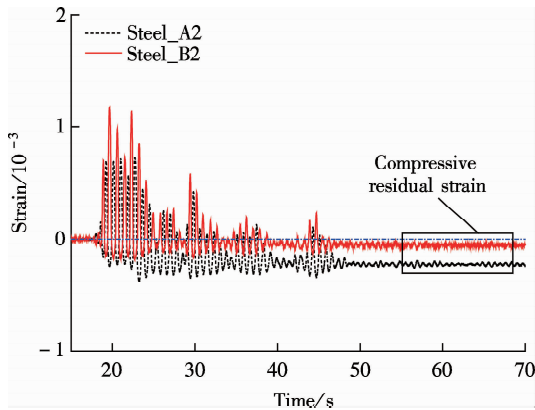


Fig. 5 Strain time-history curve of column C-S12 at A2 (input PGA = 140 cm/s^2)

The peak strain and residual strain of C-S12 are presented in Fig. 6, which shows that the residual strain is caused by the current input ground motion, and the impact of cumulative residual strain is excluded. The other columns are processed similarly.

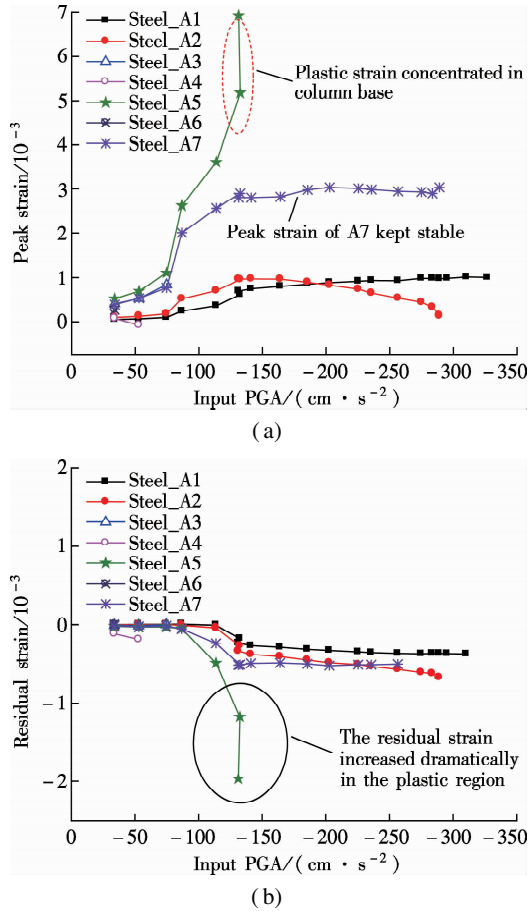


Fig. 6 Peak and residual strains of C-S12 on side A. (a) Peak strain; (b) Residual strain

In the elastic stage, the peak strain substantially increases linearly with the increase of the input PGA. For the 5th strain gauge, the residual strain significantly increases with the development of the plastic tensile strain; i. e., the plastic strain of RC column increases dramatically due to the elastoplastic property of the steel bar. The peak strain of strain gauge A7 remains stable after 3×10^{-3} , and for B7, the peak strain remains stable after 2.5×10^{-3} . Subsequently, with the increase of the input PGA, the increased energy is absorbed by the plastic deformation in the plastic hinge.

The peak strains of the longitudinal reinforcement of C-S10B85 are shown in Fig. 7. The strain gauge A1 in the anchorage zone has the minimum peak strain, which

is similar to the trend of C-S12. From the bottom of C-S10B85, the peak strain decreases with the increase of the distance from the column platform; when A7 has the highest position, the corresponding peak strain is smaller. It is observed that the strain gauge A2 (in the anchorage region) has a higher peak strain than that of C-S12, and the A6 peak strain is even higher than that of A5, indicating that the outer BFRP of the SFCB has a restrictive effect on the inner steel bar, and the plastic strain is more uniform than that of C-S12.

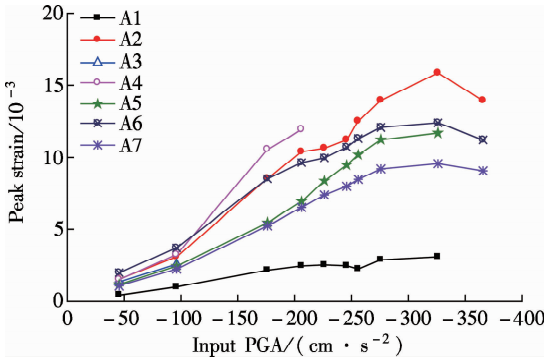


Fig. 7 The peak strain of C-S10B85

The peak strain responses of the FRP bars in C-H are illustrated in Fig. 8. The distribution of the peak strain of the FRP bar is found to have a high degree of accordance with the moment distribution. For example, strain gauge A3 (at the interface of the column base and platform) has the highest peak strain. The residual strains of the FRP bars are similar to those of C-S10B85, which are not presented.

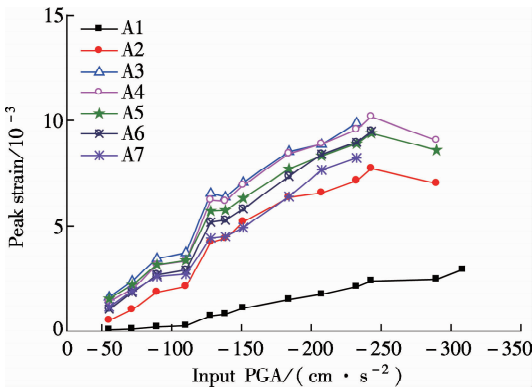


Fig. 8 The peak strain of the FRP bar in C-H

Generally, the peak strain of the steel bar in C-H is similar to that of the FRP bar due to the section deformation compatibility. However, the plastic strain of the steel bar is more concentrated in the base of the column, and the plastic strain of the FRP bar is more evenly distributed. For example, the steel strain is higher than that of the FRP strain at the interface between the column base and the platform ($S3 > A3$); the peak strain in the steel bar is lower than that of FRP bar away from the column base ($S7 < A7$).

The residual strain of the steel bar in column C-H is

shown in Fig. 9. When the input PGA is about 100 cm/s^2 , the residual strain of T3 is about -8.5×10^{-4} , and the residual strain of the symmetrical side (S5) is relatively small. With the loading progresses (after the input PGA reaches 175 cm/s^2), the residual value of T3 becomes a tensile strain, and the residual strain of S5 on the corresponding symmetrical side becomes a compressive strain. The differences in the residual strain may be caused by the following reasons: 1) The cracking of the cross-section has a closed trend due to the axial weight, and the residual tensile strain in the steel bar has a compressive effect on the adjoining area; 2) After the partial spalling of the concrete cover, the buckled steel bar has a squeezing effect on the adjacent area.

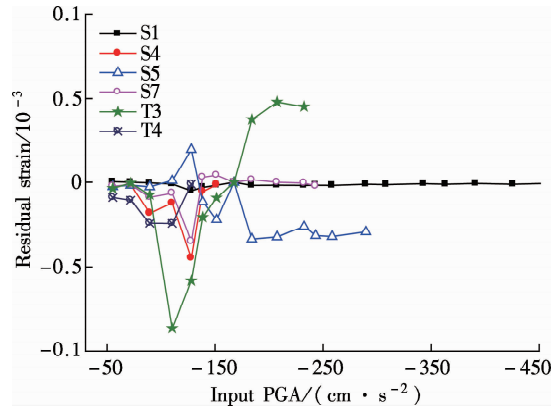


Fig. 9 The residual strain of the steel bar in C-H

The relative values of the peak strain in the anchorage region of A1 and A2 are the peak strain gauge positions: $C-S12_{\text{peak}} < C-H_{\text{FRP_peak}} < C-S10B85_{\text{peak}}$. The reason is that, the ultimate strain of the steel bar in C-S12 is smaller than that of the FRP bar in C-H, whereas the bond performance of S10B85 is better than that of the FRP bar due to the bigger interface between S10B85 and surrounding concrete. From the strain data above the column platform (A4-A7), the strain of C-S10B85 is slightly higher than that of the FRP bar (A4, A6) in C-H, whereas A7 of C-S10B85 is lower than that of the FRP bar of C-H.

3 Conclusions

1) The absolute acceleration responses of the three columns are similar to each other. Regarding the absolute PGA response, the concrete block has the relative maximum value when the input PGA of the ground motion is small, and it becomes the comparatively largest value after concrete cracking or spalling. The relative PGA response of the concrete block maintains the relative highest value throughout the test.

2) The residual strain in the anchorage region can be compression or tension, depending on the type of the longitudinal reinforcement and the anchorage method. The anchorage peak strain of C-S12 is relatively small due to the elastoplastic characteristics and low strength of the steel bar.

With a similar input PGA, the peak strain of the SFCB column can reach two times that of an ordinary RC column.

3) With the increase of the input PGA, the plastic strain of C-S12 is concentrated in the column base, and the corresponding residual strain is higher than that of the hybrid reinforced column, indicating that the SFCB column can have evenly distributed peak strain in the plastic hinge and smaller residual strain. The hybrid reinforcement column is found to resist major earthquakes by steel buckling and keeping the FRP bar undamaged, thereby achieving a balance between energy absorption and post-earthquake recoverability.

References

[1] Bruneau M, Reinhorn A. Overview of the resilience concept[C]//*Proceedings of the 8th US National Conference on Earthquake Engineering*. San Francisco, CA, USA, 2006: 2040-1 – 2040-9.

[2] Priestley M J N. Performance based seismic design[J]. *Bulletin of the New Zealand Society for Earthquake Engineering*, 2000, **33**(3): 325 – 346.

[3] Ye L P, Lu X Z, Ma Q L, et al. Influence of post-yielding stiffness to seismic response of building structures[J]. *Journal of Building Structures*, 2009, **30**(2), 17 – 29. (in Chinese)

[4] Wu G, Wu Z S, Luo Y B, et al. A new reinforcement material of steel fiber composite bar (SFCB) and its mechanics properties[C/CD]//*Proceedings of 9th International Symposium on Fiber Reinforced Polymer Reinforcement for Concrete Structures*. Adelaide, Australia, 2009: 00209-1 – 00209-4.

[5] Wu G, Wu Z S, Luo Y B, et al. Mechanical properties

of steel-FRP composite bar under uniaxial and cyclic tensile loads[J]. *Journal of Materials in Civil Engineering*, 2010, **22**(10): 1056 – 1066. DOI: 10.1061/(asce)mt.1943-5533.0000110.

[6] Sun Z Y, Yang Y, Qin W H, et al. Experimental study on flexural behavior of concrete beams reinforced by steel-fiber reinforced polymer composite bars[J]. *Journal of Reinforced Plastics and Composites*, 2012, **31**(24): 1737 – 1745. DOI: 10.1177/0731684412456446.

[7] Sun Z Y, Wu G, Wu Z S, et al. Seismic behavior of concrete columns reinforced by steel-FRP composite bars[J]. *Journal of Composites for Construction*, 2011, **15**(5): 696 – 706. DOI: 10.1061/(asce)cc.1943-5614.0000199.

[8] Ibrahim A I, Wu G, Sun Z Y. Experimental study of the cyclic behavior of concrete bridge columns reinforced by steel-basalt fiber composite bars and hybrid stirrups[J/OL]. *Journal of Composites for Construction*, (2016-08-17) [2016-10-09]. [http://dx.doi.org/10.1061/\(ASCE\)CC.1943-5614.0000742](http://dx.doi.org/10.1061/(ASCE)CC.1943-5614.0000742).

[9] Li J, Gong J. Seismic strengthening of reinforced concrete columns damaged by rebar corrosion using combined CFRP and steel jacket[J]. *Journal of Southeast University (English Edition)*, 2009, **25**(4): 506 – 512.

[10] Motaref S, Saïidi M S, Sanders D. Shake table studies of energy-dissipating segmental bridge columns[J]. *Journal of Bridge Engineering*, 2014, **19**(2): 186 – 199. DOI: 10.1061/(asce)be.1943-5592.0000518.

[11] Sun Z Y, Wu G, Wu Z S, et al. Nonlinear behavior and simulation of concrete columns reinforced by steel-FRP composite bars[J]. *Journal of Bridge Engineering*, 2014, **19**(2): 220 – 234. DOI: 10.1061/(asce)be.1943-5592.0000515.

地震作用下钢-FRP 复合配筋混凝土柱试验研究

孙泽阳¹ 吴 刚¹ 王燕华¹ 吴智深^{1,2}

(¹ 东南大学混凝土及预应力混凝土结构教育部重点实验室, 南京 210096)
(² 东南大学城市工程科学技术研究院, 南京 210096)

摘要: 为了研究复合配筋混凝土柱的动力响应性能特征,进行了等初始刚度的普通钢筋混凝土(RC)柱、钢-连续纤维(FRP)复合筋(SFCB)混凝土柱和混杂配筋混凝土柱(钢筋/FRP筋,C-H)振动台试验. 研究结果表明,不同配筋混凝土柱的加速度峰值响应差别不大;RC柱在柱台输入波峰值加速度达到100 cm/s²之后,塑性铰区钢筋塑性应变快速发展,且有较大震后残余应变;SFCB柱在纵筋峰值应变达到0.015时,相应残余应变依然在5×10⁻⁴以下;C-H柱具有和SFCB柱类似的残余应变较小的优势. 总体而言,在普通环境下混杂配筋柱可以实现较小的震后残余应变,而SFCB混凝土柱具有较高的震后可修复性(较小残余位移)的同时,可以在海洋等恶劣环境下具有高耐久性.

关键词: 混凝土柱;振动台试验;混杂配筋;峰值加速度;应变分布

中图分类号: TU375.3